Casting Solvent Effect on Crystallization Behavior of Poly(vinyl acetate)/Poly(ethylene oxide) Blends: DSC Study

W. B. WU,[1] W. Y. CHIU,[1] AND W. B. LIAU[2]

[1]Department of Chemical Engineering, National Taiwan University, Taipei, Taiwan

[2]Institute of Materials Science and Engineering, National Taiwan University, Taipei, Taiwan

Received 11 March 1996; accepted 8 September 1996

ABSTRACT: Poly(vinyl acetate) (PVAc)/poly(ethylene oxide) (PEO) blends were prepared by casting from either benzene or chloroform. The solvent effects on the crystallization behavior and thermodynamic properties of the blends were studied by the differential scanning calorimeter (DSC). Two grades of PEO with different molecular weights (PEO200 with M_w = 200,000 g/mol and PEO2 with M_n = 2000 g/mol) were used in this work. The thermal analysis revealed that the blends cast from either benzene or chloroform were miscible in the molten state. The crystallization of PEO in the benzene-cast blends was more easily suppressed than it was in the chloroform-cast blends. Furthermore, the benzene-cast blends showed a greater negative value of Flory-Huggins interaction parameter than those cast from chloroform in the PVAc/PEO200 polyblend system. It was supposed that the benzene-cast blends had more homogeneous morphology. © 1997 John Wiley & Sons, Inc. J Appl Polym Sci **64:** 411–421, 1997

Key words: poly(vinyl acetate); poly(ethylene oxide); blend; miscibility; solvent effect; crystallization; interaction parameter

INTRODUCTION

Recently, the subject of miscibility of polymer–polymer blend has gained much attention.[1,2] From the thermodynamic point of view, two components will be miscible only if the Gibbs free energy of mixing is negative. If the combinatorial entropy term is negligible for polymer blend, then it requires the exothermic heat of mixing to form a miscible blend. In other words, interact with oxygen in the ether group.[3] Polymer blends with this specific interaction include poly(methyl methacrylate) (PMMA)/poly(ethylene oxide) (PEO) and PVAc/PEO blends. The PMMA/PEO blends have been proved to be miscible and their crystallization kinetics and thermodynamic properties have been extensively studied.[4–8] The PVAc/PEO blends have been studied by the following research groups. Kalfoglou et al.[9,10] studied the miscibility of PVAc/PEO blends by means of optical microscopy (OM), dynamic mechanic analysis (DMA), and differential scanning calorimeter (DSC). It was reported that the blends were miscible at high PVAc compositions. Martuscelli and Silvestre et al.[11,12] studied the crystallization behavior, thermodynamic properties, and morphology of these blends by using OM, DSC, and small angle X-ray scattering (SAXS). They found that the spherulite growth rate and the overall kinetic rate constant of crystallization decreased with increasing the PVAc content. Additionally, the blends were granted to be miscible from the observation of their single glass transition temperature (T_g) behavior. From the SAXS

Correspondence to: W. B. Liau.

analysis, it was revealed that the PVAc existed not only in the interlamellar zone but also in the interfibrillar zone. Munoz et al.[13] studied the rheological properties and thermodynamic properties of these blends. It was reported that the viscosity of the blend decreased with increasing the PEO content. The polymer–polymer interaction parameter (χ) was found to be -0.08 at 70°C from the depression of melting point. Han, Chung, and Kim[14] studied the phase behavior of these blends. They reported that the PVAc/PEO20 (M_w of PEO = 20,000) blends were miscible but two T_g values were found in the high PVAc compositions of PVAc/PEO100 (M_w of PEO = 100,000) blends. The values of χ were -0.211 and -0.069 for the PVAc/PEO20 and PVAc/PEO100 blends, respectively. In the above two articles, non-equilibrium melting points were used to estimate the value of χ. Yin et al.[3] studied the miscibility of PVAc/PEO blends from the heat-of-mixing data, which were evaluated by measuring the heats of solution of pure components and blends in a common solvent and applying Hess's law. It was reported that a negative heat of mixing was found in blends of PEO and low molecular weight PVAc. Using the experimental data to fit the Patterson theory[15] of polymer–polymer miscibility led to the results that the free-volume term had a much smaller value than the interaction one.

Owning to the high viscosity of polymer, true equilibrium is difficult to reach for polymer blends. Therefore, the physical properties of polymer blends are usually influenced by their history (including the heat treatment and prepared methods). Bank, Leffingwell, and Thies[16] investigated the solvent effect on the miscibility of polystyrene (PS)/poly(vinyl methyl ether) (PVME) blends. It was concluded that the compatible PS/PVME blends were obtained upon casting from toluene or benzene, while incompatible blends upon casting from chloroform. In the literature, many amorphous/crystalline polymer blends have proven to be miscible in the molten state by the thermal analysis, such as PEI/PEEK,[17] PAr/PBT,[18] PMMA/PVDF,[19] and amorphous/PEO[3,4,8–15,20–22] blends. To our knowledge, limited papers studying the prepared method or solvent effect on the properties of amorphous/crystalline polymer blends were published.[23,24] For the PVAc/PEO blends, chloroform was the only solvent used for preparing blends in all papers reviewed in the above.[9–14] In this work, the non-polar solvent, benzene, as well as the polar solvent, chloroform, was used to study the casting solvent effect on the crystallization behavior and thermodynamic properties of PVAc/PEO blends.

There is a certain relationship between the miscibility and Flory-Huggins interaction parameter of the polymer blend. The common methods employed to evaluate the value of interaction parameter include melting-point depression, vapor sorption, inverse-phase gas chromatography, neutron scattering, and small-angle X-ray scattering. Each method has some advantages and disadvantages.[25] For a compatible amorphous/crystalline polymer blend, the polymer–polymer interaction parameter was usually estimated from the depression of the melting point of crystalline polymer by using the Nish-Wang equation.[19] Although there was some dispute about this method,[26,27] it was still the favorite one. In this work, equilibrium melting points were used to estimate the polymer–polymer interaction parameter of PVAc/PEO blends.

EXPERIMENTAL

Materials and Blend Preparation

The materials used in this work and their characteristics were given in Table I. All PEO molecules were terminated with hydroxyl groups. Certain amounts of PVAc and PEO were dissolved in benzene (or chloroform) according to the desired composition. The total polymer concentration was 1 g/p 100 mL solvent. The solution was continuously stirred for 2 days at room temperature and then poured onto the glass plate. The solvent was evaporated slowly under ambient condition at 30°C. Finally, the blend film of $\sim$ 0.08 mm in thickness was obtained. The sample film or chip was dried in the vacuum oven at 45°C for at least 1 week in order to remove the residual solvent (more time required for benzene-cast blends).

Glass Transition Temperature (T_g) Measurement

Glass transition temperature (T_g) measurements were carried out by using a Du Pont differential scanning calorimeter (model 9900). Indium (melting point, T_m = 156.6°C) and n-heptane (T_m = -90.6°C) were used as standards for temperature calibration. Samples of $\sim$9 mg loaded in aluminum cells were heated to 100°C for 10 min to melt PEO crystals, followed by quenching to -130°C and then scanned to 100°C with a heating rate 20°C/min. T_g was determined from the half-

Table I Materials and Their Characteristics

Code	Description	Source
PVAc	Poly(vinyl acetae), M_w = 260,000	Scientific Polymer Products, Inc.
PEO200	Poly(ethylene oxide), M_w = 200,000	Scientific Polymer Products, Inc.
PEO2	Polyethylene glycol, M_n = 2000	Merck

height point of the step change in the thermogram and the error was within 2°C. The second and third runs were also analyzed and the results were very similar to the first run.

Isothermal Crystallization Analysis and Melting Temperature (T_m) Measurement

The isothermal crystallization experiments were carried out by using a Perkin-Elmer differential scanning calorimeter (model DSC-7). Indium (T_m = 156.6°C) and *n*-octadecane (T_m = 28.2°C) were used for temperature calibration. About 6 mg of sample was heated to 90°C to melt crystals, and then cooled to a specified crystallization temperature (T_c) at a cooling rate of 60°C/min under helium purge and ice water surrounding condition. After the completion of crystallization, the sample was heated to 90°C with a scanning rate of 10°C/min. The melting temperature was defined as the maximum point of endothermic peak. When certain samples were repeatedly run, it seemed that T_m was almost independent of number of cycles at a certain T_c for any composition. The error was within 0.15°C in this part of experiment.

RESULTS AND DISCUSSION

T_g Measurement of PVAc/PEO200 Blend

DSC thermograms of the PVAc/PEO200 blends cast from benzene were presented in Figure 1. There was a sharp thermal transition at ~ 44°C for the pure PVAc. This transition was the so-called glass transition. The pure PEO was a highly crystallized polymer, and showed a melting temperature ~66°C. The blend with 90 wt % PVAc, as well as the pure PVAc, was granted to be completely amorphous because of no melting peak in the thermograms. The thermograms of blends with 50–80 wt % PVAc exhibited exothermic peaks following the glass transitions. This indicates that recrystallization occurred in these blends. The total recrystallization heat (ΔH_{rc}), and fusion heat (ΔH_f) of the PEO200 in the blend was obtained by integrating the areas under the recrystallization and melting peaks of DSC curve, respectively. The results were listed in Table II. The blends with 60–80 wt % PVAc showed that the ΔH_{rc} was almost equal to the ΔH_f. This indicates that PVAc was sufficient to completely suppress the crystallization of PEO200 in the blend during the quenching process. For the above blends, a single T_g decrease with increasing the PEO content was found. This means that the blends were miscible in the molten state. It was difficult to quantitatively discuss the breadth of the glass transition, because the recrystallization

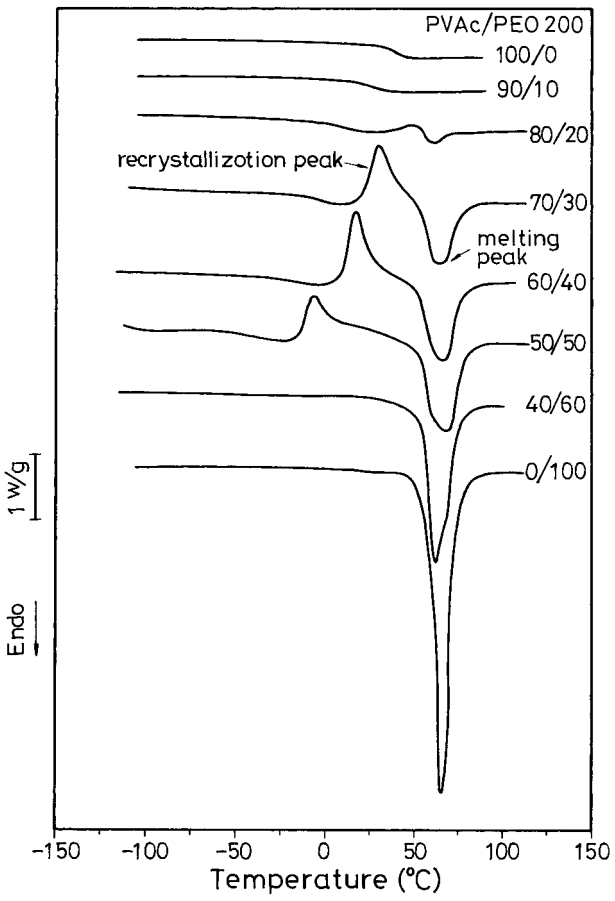

Figure 1 DSC thermograms of PVAc/PEO200 blends cast from benzene.

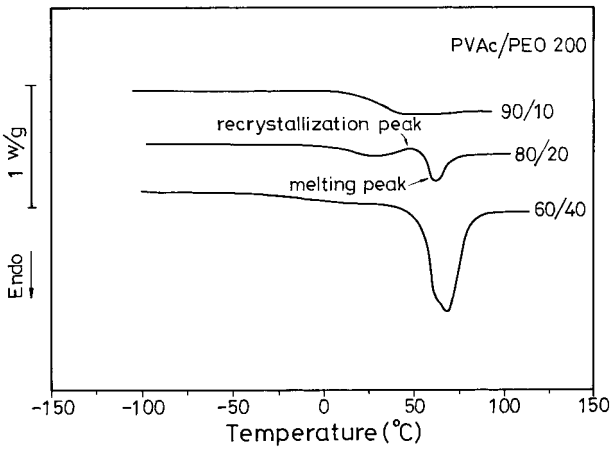

Figure 2 DSC thermograms of PVAc/PEO200 blends cast from chloroform.

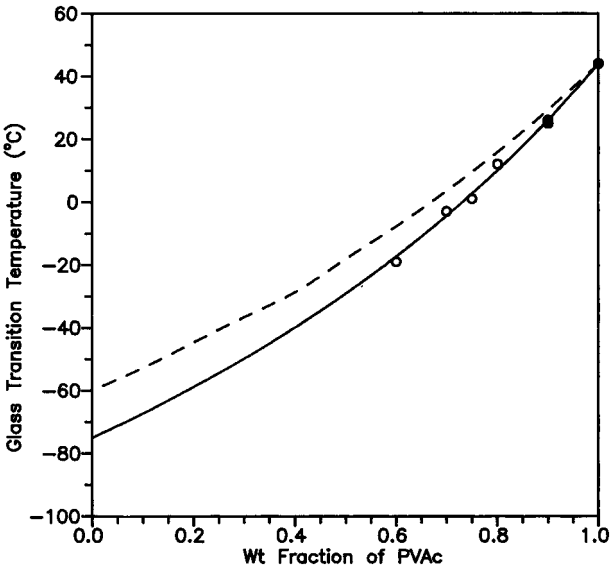

Figure 3 Glass transition temperature versus weight fraction of PVAc plot for the PVAc/PEO200 blends: (---) Fox equation, assuming T_g of PEO = −60°C; (——) Fox equation, assuming T_g of PEO = −75°C; (○), experimental data for blends cast from benzene; (●), experimental data for blends cast from chloroform.

occurred immediately after the glass transition. However, the glass transitions of the blends were much broader than that of pure PVAc. This indicates that a wide distribution of molecular environment existed in the blend, although the blends were macroscopically homogeneous. The recrystallization heat was slightly lower than the fusion heat for the blend with 50 wt % PVAc (see Table II). This indicates that some PEO200 crystallized during the quenching process, but most PEO200 remained in the amorphous phase. The single T_g means that the amorphous phase was miscible and it was corresponding to the amorphous phase composition, not the overall composition. When the PVAc content was less than 40 wt %, PVAc could hardly suppress the crystallization of PEO200 during the quenching process. For these compositions, the amorphous phase was the minor phase, and the T_g was ambiguous.

Table II Fusion Heat (ΔH_f) and Recrystallization Heat (ΔH_{rc}) or PVAc/PEO200 Blends Shown in Figure 1 and Figure 2

PVAc/PEO200	Casting Solvent	ΔH_f (J/gram of PEO200)	ΔH_{rc} (J/gram of PEO200)
100/0	benzene	—[a]	—
90/10	benzene	—	—
80/20	benzene	18	18
70/30	benzene	105	105
60/40	benzene	111	108
50/50	benzene	120	102
40/60	benzene	132	—
0/100	benzene	136	—
90/10	chloroform	—	—
80/20	chloroform	29	11
60/40	chloroform	114	—

[a] —, Very small or not obtained.

DSC thermograms for the PVAc/PEO200 blends cast from chloroform were presented in Figure 2. The fusion and recrystallization heat of these blends were also listed in Table II. The blend with 90 wt % PVAc was still completely amorphous with a single T_g. The recrystallization heat was much less than the fusion heat for the blend with 80 wt % of PVAc. (see Table II). This indicates that the crystallization of PEO200 could not be as completely suppressed as the blend cast from benzene during the quenching process. Furthermore, the fusion heat for the blend with 80 wt % PVAc was larger than that cast from benzene. That is, the crystallinity of the blend was larger than that cast from benzene. When the PEO200 content was more than 40 wt %, most PEO200 crystallized during the quenching process. In comparison of Fig. 1 to Fig. 2, it was obvious that PVAc showed better ability to suppress the crystallization of PEO200 in the blend cast from benzene. This might result from the morphology of benzene-cast blends, which was more homogeneous than that of chloroform-cast blends. When the PVAc was less than 40 wt %, the ther-

mograms and ΔH_f of the blends cast from chloroform or benzene were similar.

Figure 3 showed the relationship between the T_g and composition of PVAc/PEO200 blends. For the PEO-rich blends, completely amorphous morphology was not achieved by the quenching process. Therefore, the T_g was corresponding to the amorphous phase composition, not the overall composition, and it became obscure when the PVAc content was less than 50 wt %. Thus, their T_g values were not shown in this figure. The experimental value of T_g of pure PEO was reported to be in the range -45 to -60°C in the literature.[4,7,9–11,14,20,28,29] The dashed line in this figure represented the theoretical values of T_g calculated from the Fox equation by assuming the T_g of amorphous PEO was -60°C. The Fox equation was given as:[30]

$$\frac{1}{T_g} = \frac{W_1}{T_{g,1}} + \frac{W_2}{T_{g,2}} \qquad (1)$$

where T_g, $T_{g,1}$ and $T_{g,2}$ were the glass transition temperatures of the blend, pure component 1 and 2, respectively; W_1 and W_2 were the weight fractions of component 1 and 2 in the blend. It was found that the experimental value of T_g of the blend was lower than the theoretical one. Actually, PEO was very facile to crystallize, thus using the experimental value of T_g of PEO with high crystallinity to represent the T_g of amorphous PEO was improper. The solid line in Figure 3 represents the fitting curve of the experimental T_g values of the blends with the Fox equation. The T_g of pure amorphous PEO was then estimated to be -75°C, which was lower than that of PEO with high crystallinity.

Isothermal Crystallization Behavior and Melting Point Depression of PVAc/PEO200 Blend

The isothermal crystallization behavior of benzene- or chloroform-cast PVAc/PEO200 blend was analyzed by DSC. The time required to finish 50% crystallization was called half-time of crystallization and denoted as $t_{1/2}$. Table III showed the $t_{1/2}$ values of the pure PEO200 and its blends. As seen in general miscible amorphous/crystalline blends, the $t_{1/2}$ value increased with raising the amorphous content at any crystallization temperature. It was noted that the blends cast from benzene showed larger values of $t_{1/2}$ than those cast from chloroform. This confirmed to us that PVAc showed a better ability to reduce the crystallization rate of PEO200 in the benzene-cast blends. Figure 4 (a) and 4 (b) showed the plots of melting temperature (T_m) versus crystallization temperature (T_c) of benzene- and chloroform-cast PVAc/PEO200 blends, respectively. It was found that the T_m decreased with the increasing content of PVAc. On the other hand, the blends cast from benzene showed a more obvious depression of T_m. Hoffman and Weeks[31] suggested the relation of T_m and T_c as the following equation:

Table III $t_{1/2}$ (min) at Various T_c for PVAc/PEO200 Blends Cast from Benzene or Chloroform

T^c	Composition		
	100 wt % PEO	90 wt % PEO	60 wt % PEO
53°C	3.2	3.3[a] (6.5)[b]	6.3 (—)[c]
50°C	1.0	1.1 (1.9)	1.8 (12.3)
48°C	0.5	0.5 (0.9)	1.0 (6.2)

[a] Value not in parentheses corresponding to blend cast from chloroform.
[b] Value in parentheses corresponding to blend cast from benzene.
[c] Value not obtained.

$$T_m = T_m^\circ \left(1 - \frac{1}{\gamma}\right) + \frac{T_c}{\gamma} \qquad (2)$$

where T_m was the melting temperature of a sample crystallized at temperature T_c, T_m° was the equilibrium melting temperature, γ was the morphological factor, and meant the ratio of the lamellar thickness to the thickness of the initial nucleus. The T_m versus T_c curves in Figure 4 (a) and 4 (b) were not linear at high undercoolings. This might be ascribed to the crystal annealing, and thus thickening during the heating process to melt crystals.[27,32] The equilibrium melting point for each blend could be obtained by the linear extrapolation of the low undercooling data to the $T_m = T_c$ line. It seemed that the extrapolated lines of the blends were parallel to that of plain PEO200, that is, the morphological factor (γ) obtained from the reciprocal of slope was independent of the blend composition with a value ~ 2.4. Nish and Wang[19] have derived the equilibrium melting point of a miscible blend as a function of composition from thermodynamic consideration as the following equation:

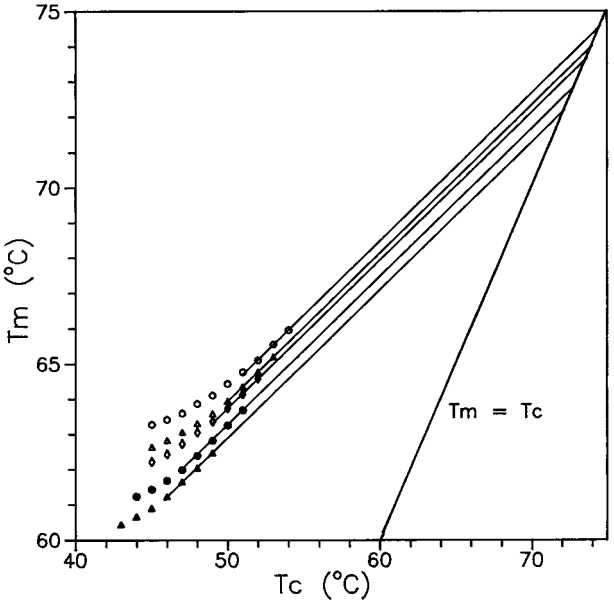

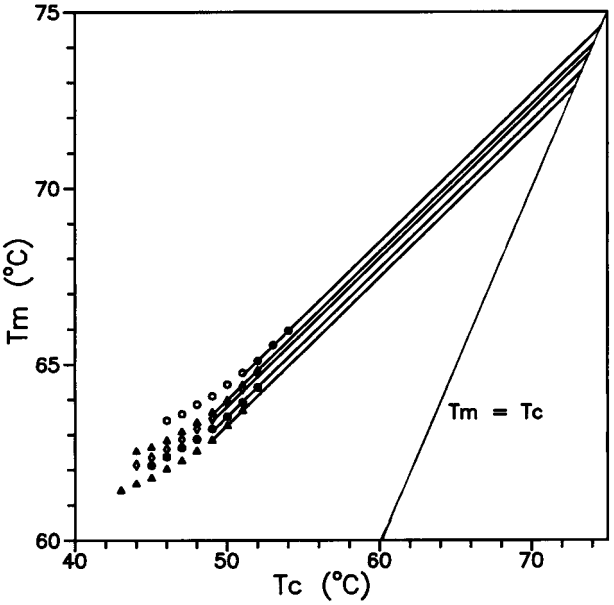

Figure 4 (a) The Hoffman-Weeks plots for the PVAc/PEO200 blends cast from benzene with: (○), 100 wt % PEO; (△), 90 wt % PEO; (◇), 75 wt % PEO; (●) 60 wt % PEO; (▲), 50 wt % PEO. (b) The Hoffman-Weeks plots for the PVAc/PEO200 blends cast from chloroform with: (○), 100 wt % PEO; (△), 90 wt % PEO; (◇), 75 wt % PEO; (●), 60 wt % PEO; (△), 50 wt % PEO.

$$\frac{1}{T_{m,b}} - \frac{1}{T_{m,p}} = -\frac{RV_{2\mu}}{\Delta H_{2\mu} V_{1\mu}}\left[\frac{\ln(1-\phi_1)}{m_2} + \left(\frac{1}{m_2} - \frac{1}{m_1}\right)\phi_1 + \chi\phi_1^2\right] \quad (3)$$

where R was the universal constant, $T_{m,p}$ was the equilibrium melting temperature of pure crystalline polymer, $T_{m,b}$ was the equilibrium melting temperature of a blend; ϕ_1 was the volume fractions of amorphous polymer, $H_{2\mu}$ was the heat of fusion per mole of repeated unit of perfect crystalline polymer, $V_{1\mu}$ and $V_{2\mu}$ were the molar volumes of the repeated units of the amorphous and crystalline polymers, respectively; m_1 and m_2 were the degrees of polymerization for the amorphous and crystalline polymers, respectively. χ was the polymer–polymer interaction parameter and could be written in the following form:[19]

$$\chi = \frac{BV_{1\mu}}{RT} \quad (4)$$

where B was the interaction energy density characteristic of the polymer pair. Substituting eq. (4) into eq. (3) gave:

$$-\left\{\frac{\Delta H_{2\mu}}{V_{2\mu}}\left(1 - \frac{T_{m,b}}{T_{m,p}}\right) + \frac{RT_{m,b}}{V_{1\mu}}\left[\frac{\ln(1-\phi_1)}{m_2} + \left(\frac{1}{m_2} - \frac{1}{m_1}\right)\phi_1\right]\right\} = B\phi_1^2 \quad (5)$$

For high molecular weight polymers, eq. (5) could be simplified as:

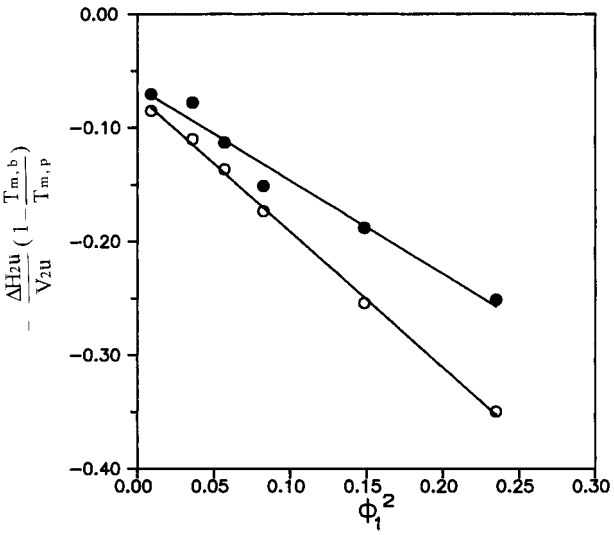

Figure 5 Plot of eq. (6) to obtain interaction parameter of PVAc/PEO200 blends: (○), cast from benzene; (●), cast from chloroform.

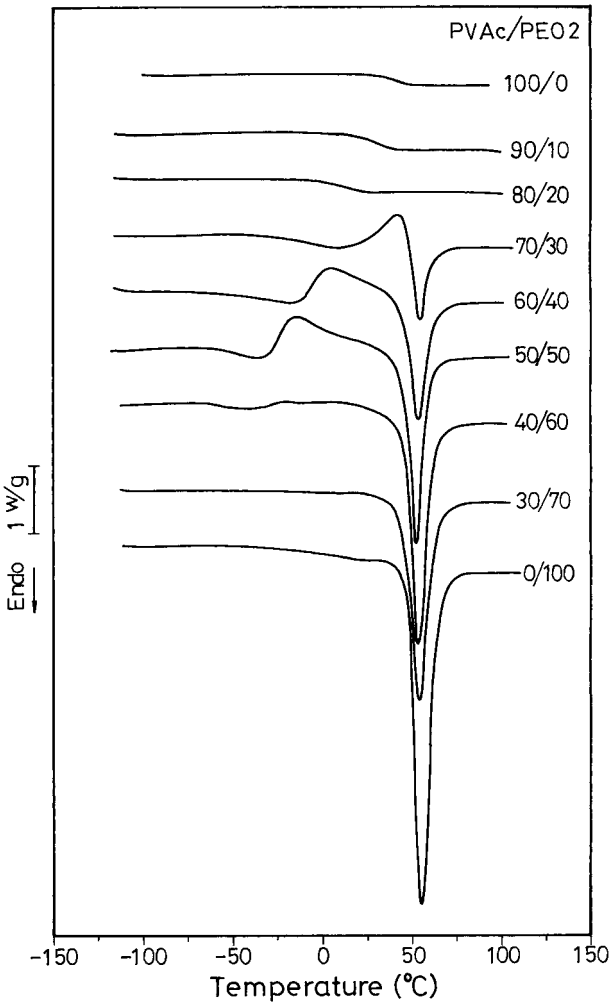

Figure 6 DSC thermograms of PVAc/PEO2 blends cast from benzene.

$$-\frac{\Delta H_{2\mu}}{V_{2\mu}}\left(1-\frac{T_{m,b}}{T_{m,p}}\right)=B\phi_1^2 \qquad (6)$$

B could be obtained from the slope of the left-hand side terms of eq. (6) versus ϕ_1^2 plot. In fact, thermal equilibrium was difficult to reach for high polymer blends. In the literature, many well-known formulae had been used under non-equilibrium, although they were derived from the concept of equilibrium. This would lead to the result that the B value obtained from using eq. (6) was not a true equilibrium, but one depending on the history of blending. For PVAc/PEO200 polyblend system, $V_{1\mu}$ = 74.5 cm^3/mol,[33] $V_{2\mu}$ = 40.5 cm^3/mol,[6] and $\Delta H_{2\mu}$ = 2070 cal/mol,[34] the value of B was estimated to be −1.20 for the blends cast from benzene and −0.82 for those cast from chloroform, as shown in Figure 5. The corresponding value of χ was −0.13 for the benzene-cast blends and −0.09 for the chloroform-cast blends at 70°C. The negative value of χ confirmed the miscibility of PEO-rich blends in the molten state. It was found that the intercepts were not zero for both blends, perhaps resulting from the residual entropy effect.[35,36] The benzene-cast blend had a greater negative interaction parameter, in other words, more heat was released upon mixing. This was also ascribed to the more homogeneous morphology of blend cast from benzene.

T_g Measurement of PVAc/PEO2 Blend

The molecular weights of PVAc and PEO discussed above were 260,000 g/mol and 200,000 g/mol, respectively. Although the blends were maintained at a temperature higher than the T_m of PEO and T_g of PVAc for a period of time before any thermal test, the crystallization behavior and interaction parameter of the blends were still influenced by their history (casting solvent). This might result from the high viscosity and low diffusivity of the blend. Therefore, we selected a low molecular weight PEO (M_n = 2000 g/mol, PEO2) replacing PEO200 to be blended with PVAc. Then the crystallization behavior and thermodynamic properties of these blends were analyzed.

DSC thermograms of PVAc/PEO2 blends cast from benzene were presented in Figure 6. The fusion heat and recrystallization heat of these blends were listed in Table IV. The blends with 80–90 wt % PVAc were complete amorphous. Thermograms of blends with 40–70 wt % PVAc showed obvious recrystallization peaks following the glass transition, but only those with 50–70 wt % PVAc showed an almost equal amount of recrystallization heat and fusion heat. In other words, when the blends contained PVAc more than 50 wt %, the crystallization of PEO2 was completely suppressed by the quenching process. For the above blends, a single T_g decreased with increasing PEO2 content was found. This indicates that these PVAc/PEO2 blends were miscible in their molten state. When the PVAc content was less than 30 wt %, the PVAc could hardly suppress the crystallization of PEO2, and most PEO2 crystallized during the quenching process.

DSC thermograms of PVAc/PEO2 blends cast from chloroform were presented in Figure 7. The fusion heat and recrystallization heat of these blends were also listed in Table IV. The thermograms were similar to those cast from benzene

except for the blends with 80 wt % and 70 wt % PVAc. The blend with 80 wt % PVAc was not completely amorphous and the recrystallization heat was equal to the fusion heat. The blend with 70 wt % PVAc showed larger recrystallization heat and fusion heat than those cast from benzene. ($\Delta H_f = \Delta H_{rc} = 87$ J per gram PEO2 for benzene-cast blend and $\Delta H_f = \Delta H_{rc} = 113$ J per gram PEO2 for chloroform-cast blend.) This also indicated that the crystallization of PEO2 was more easily suppressed in the benzene-cast blends, but the trend was not as obvious as the PVAc/PEO200 system.

In comparison with the thermograms of PVAc/PEO2 and PVAc/PEO200 blends cast from benzene, it was found that the PVAc/PEO2 blend with 80 wt % PVAc was completely amorphous but the PVAc/PEO200 blend with 80 wt % PVAc showed crystallization behavior. Furthermore, the PVAc/PEO2 blend with 40 wt % PVAc showed obvious recrystallization behavior. More directly, the crystallization of PEO2 was partially suppressed during the quenching process. However, the corresponding composition of PVAc/PEO200 blends did not recrystallize. It seemed PVAc showed better ability to suppress the crystallization of PEO in the polyblend system with lower molecular weight of PEO. This may be attributed to the higher degree of mixing in the PVAc/PEO2 system. Similar results were also found in the chloroform-cast blends.

Figure 8 showed the relation relationship between the T_g and composition of PVAc/PEO2 blends. It seemed that the solvent effect on the values of T_g of the blends was not clear because the difference was within the extent of error. The T_g of amorphous PEO2 was estimated to be −98°C by using the Fox equation to fit the experimental data. This value was 25°C lower than that of PEO200. It seemed that the T_g of amorphous PEO was significantly molecular weight-dependent in this molecular weight range.

Isothermal Crystallization Behavior and Melting Point Depression of PVAc/PEO2 Blend

The isothermal crystallization behaviors of PVAc/PEO2 blends were also analyzed. The half-time of crystallization ($t_{1/2}$) of blends cast from either benzene or chloroform were listed in Table V. For all blends at a given crystallization temperature, benzene-cast blends still showed more obvious reduction of overall crystallization rates. In comparison of the data of blends with 60 wt % PEO in

Table IV Fusion Heat (ΔH_f) and Recrystallization Heat (ΔH_{rc}) of PVAc/PEO2 Blend Shown in Figure 6 and Figure 7

PVAc/PEO2	Casting Solvent	ΔH_f (J/gram of PEO2)	ΔH_{rc} (J/gram of PEO2
100/0	benzene	—[a]	—
90/10	benzene	—	—
80/20	benzene	—	—
70/30	benzene	87	87
60/40	benzene	140	138
50/50	benzene	140	133
40/60	benzene	153	40
30/70	benzene	158	—
0/100	benzene	160	—
100/0	chloroform	—	—
90/10	chloroform	—	—
80/20	chloroform	23	23
70/30	chloroform	113	113
60/40	chloroform	142	134
50/50	chloroform	140	122
40/60	chloroform	155	43
30/70	chloroform	154	—
0/100	chloroform	158	—

[a] —, Very small or not obtained.

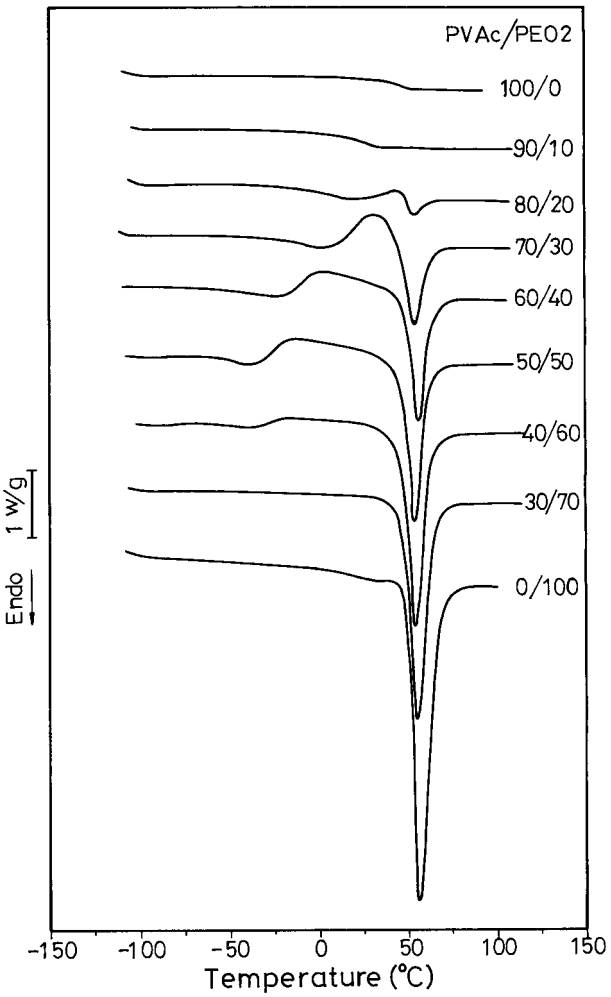

Figure 7 DSC thermograms of PVAc/PEO2 blends cast from chloroform.

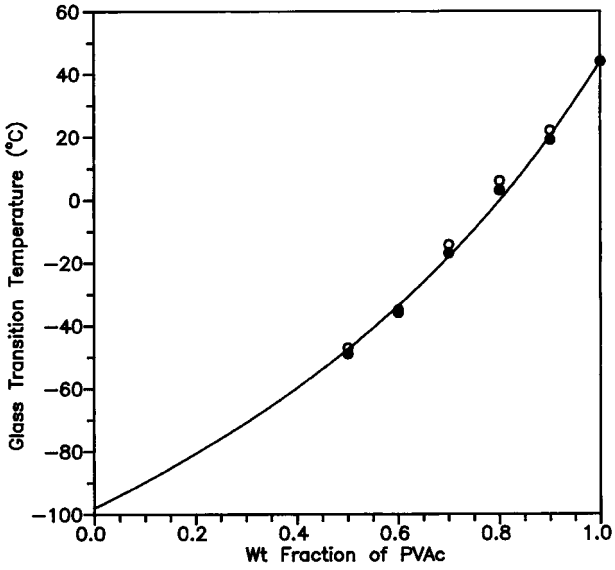

Figure 8 Glass transition temperature versus weight fraction of PVAc plot for the PVAc/PEO2 blends: (——) Fox equation, assuming T_g of PEO = −98°C; (○), experimental data for blends cast from benzene; (●), experimental data for blends cast from chloroform.

Tables III and V, it was found that the value of $t_{1/2}$ of benzene-cast blend was more than six times as much as that cast from chloroform for the PVAc/PEO200 system, but about two times for the PVAc/PEO2 system. This also indicated that the solvent effect was more obvious in the blend with high molecular weight of PEO. Figure 9 (a) and 9 (b) showed the T_m versus T_c plots of PVAc/PEO2 blends cast from benzene and chloroform, respectively. It was found that the melting temperatures of PEO2 and its blends were independent of T_c. This indicated that the crystals were extended chain crystals or crystals with the constant number of folds.[37] The equilibrium T_m was equal to the T_m at any T_c, because the slope of extrapolating line was zero. The interaction parameter of these blends could also be obtained from the Nish-Wang equation (eq. 5). Because the molecular weight of PEO2 was only 2000, the entropy contribution must be considered. The left-hand side terms of eq. (5) versus ϕ_1^2 plot was shown in Figure 10. The value of B was calculated from the slope of the fitting line to be −0.83 and the value of χ was −0.097 at 50°C. This also confirmed that the PEO-rich blends were miscible in the molten state. The solvent effect on the value of χ was unobvious in this system.

The value of B was −0.83 for the PVAc/PEO2 blends and −1.2 for the PVAc/PEO200 blends cast from benzene. It was unusual that the blend with lower molecular weight component showed

Table V $t_{1/2}$ (min) at Various T_c for PVAc/PEO2 Blends Cast from Benzene or Chloroform

	Composition		
T^c	100 wt % PEO	90 wt % PEO	60 wt % PEO
38°C	1.6	1.8[a]	6.2
		(3.6)[b]	(12.0)
36°C	0.9	0.9	2.6
		(1.6)	(4.6)
33°C	0.4	0.4	1.1
		(0.8)	(2.3)

[a] Value not in parentheses corresponding to blend cast from chloroform.

[b] Value in parentheses corresponding to blend cast from benzene.

a less negative value of B. Temperature and chain length effects would not be able to explain this result. One possible reason was the self-association effect of PEO2 molecules by way of hydroxyl end groups and the other was the error to find equilibrium melting temperature. The chain length and end group effect on the interaction parameter of PVAc/PEO blends will be studied in our future work.

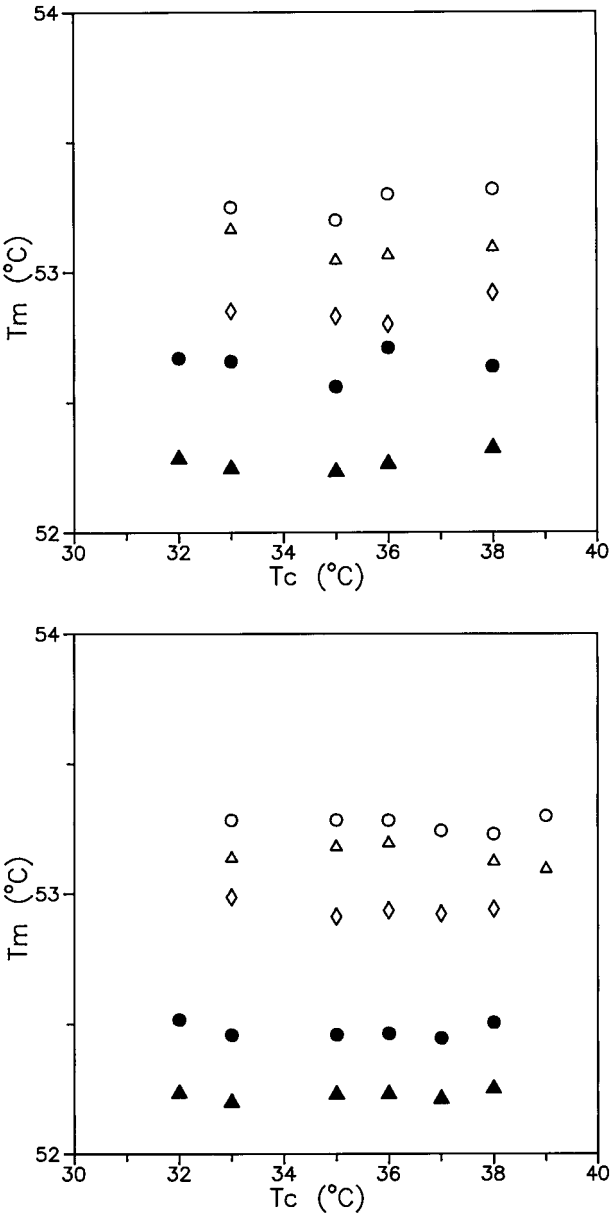

Figure 9 (a) The Hoffman-Weeks plots for the PVAc/PEO2 blends cast from benzene with: (○), 100 wt % PEO; (△), 90 wt % PEO; (◇), 80 wt % PEO; (●), 70 wt % PEO; (▲), 60 wt % PEO. (b) The Hoffman-Weeks plots for the PVAc/PEO2 blends cast from chloroform with: (○) 100 wt % PEO; (△), 90 wt % PEO; (◇), 80 wt % PEO; (●), 70 wt % PEO; (▲), 60 wt % PEO.

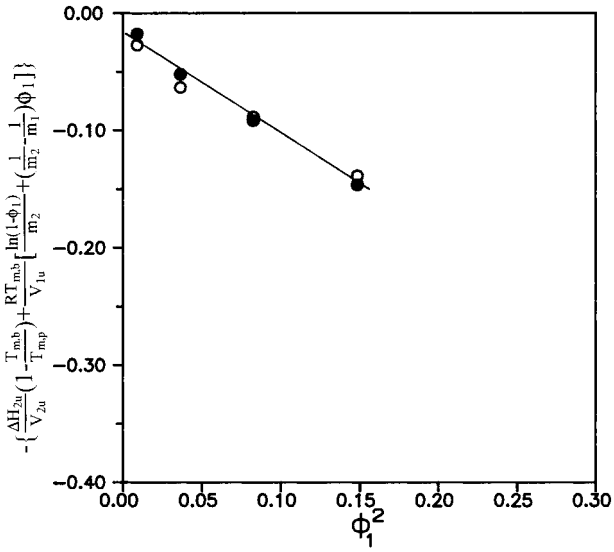

Figure 10 Plot of eq. (5) to obtain interaction parameter of PVAc/PEO2 blends: (○), cast from benzene; (●), cast from chloroform.

CONCLUSIONS

From the depression of crystallization rate and melting point of PEO in the PEO-rich blends and the single T_g in the PVAc-rich blends, it was supposed that the PVAc/PEO blends were miscible in the molten state. The crystallization of PEO was more easily suppressed in the benzene-cast blends than it was in the chloroform-cast blends. Additionally, PVAc showed better ability to suppress the crystallization of PEO in the polyblend system with lower molecular weight of PEO. For the polyblend system with high molecular weight PEO, the benzene-cast blends showed a more negative value of polymer–polymer interaction parameter than those cast from chloroform. To sum up, it was supposed that the benzene cast blends had more homogeneous morphology.

The authors acknowledge with gratitude financial support from the National Science Council, Taiwan, R.O.C., through Grant No. NSC83-0405-E-002-132.

REFERENCES

1. D. R. Paul and S. Newman, *Polymer Blends,* Academic Press, New York, 1978.

2. O. Olabisi, L. M. Robeson, and M. T. Shaw, *Polymer-Polymer Miscibility,* Academic Press, New York, 1979.
3. J. Yin, G. C. Alfonso, A. Turturro, and E. Pedemonte, *Polymer,* **34,** 1465 (1993).
4. E. Calahorra, M. Cortazar, and G. M. Guzman, *Polymer,* **23,** 1322 (1982).
5. G. C. Alfonso and T. P. Russell, *Macromolecules,* **19,** 1143 (1986).
6. S. Cimmino, E. Martuscelli, and C. Silvestre, *Polymer,* **30,** 393 (1989).
7. X. Li and S. L. Hsu, *J. Polymer. Sci. Polym. Phys. Ed.* **22,** 1331 (1984).
8. E. Martuscelli, C. Silvestre, M. L. Addonizio, and L. Amelino, *Makromol. Chem.,* **187,** 1557 (1986).
9. N. K. Kalfoglou, *J. Polym. Sci. Polym. Phys. Ed.,* **20,** 1259 (1982).
10. N. K. Kalfoglou, D. D. Sotiropoulou, and A. G. Margaritis, *Eur. Polym. J.,* **4,** 389 (1988).
11. E. Martuscelli, C. Silvestre, and C. Gismondi, *Makromol. Chem.* **186,** 2161 (1985).
12. C. Silvestre, F. E. Karasz, W. J. MacKnight, and E. Martuscelli, *Eur. Polym. J.,* **23,** 745 (1987).
13. E. Munoz, E. Calahorra, M. Cortazar, and A. Santamaria, *Polym. Bull.* **7,** 295 (1992).
14. C. D. Han, H. S. Chung, and J. K. Kim, *Polymer,* **33,** 546 (1992).
15. D. Patterson and A. Robard, *Macromolecules,* **11,** 690 (1978).
16. M. Bank, J. Leffingwell, and C. Thies, *Macromolecules,* **4,** 43 (1971).
17. B. S. Hsiao and B. B. Sauer, *J. Polym. Sci. Polym. Phys. Ed.,* **31,** 901 (1993).
18. P. P. Huo, P. Cebe, and M. Capel, *Macromolecules,* **26,** 4275 (1993).
19. T. Nish and T. T. Wang, *Macromolecules,* **8,** 909 (1975).
20. S. Cimmio, E. Martuscelli, C. Silvestre, M. Canetti, C. D. Lalla, and A. Seves, *J. Polym. Sci. Polym. Phys. Ed.,* **27,** 1781 (1989).
21. L. C. Cestreros, J. R. Quintana, J. A. Fernandez, and I. A. Katime, *J. Polym. Sci. Polym. Phys. Ed.,* **27,** 2567 (1989).
22. E. Pedemonte and G. Burgisi, *Polymer,* **35,** 3719 (1994).
23. S. Cimmino, E. D. Pace, E. Martuscelli, and C. Silvestre, *Makromol. Chem.,* **191,** 2447 (1990).
24. C. Tsitsilianis, G. Staikos, and A. Dondos, *Polymer,* **33,** 3369 (1992).
25. B. Riedl and R. E. Prud'homme, *Polym. Eng. Sci.,* **24,** 1291 (1984).
26. P. B. Rim and J. Runt, *Macromolecules,* **17,** 1520 (1984).
27. J. Runt and K. P. Gallapher, *Polym. Commun.,* **32,** 180 (1991).
28. Q. Guo, X. Peng, and Z. Wang, *Polymer,* **32,** 53 (1991).
29. C. Nakafuku and M. Sakoda, *Polym. J.,* **25,** 909 (1993).
30. T. G. Fox, *Bull. Am. Phys. Soc.,* **1,** 123 (1956).
31. J. D. Hoffman and J. J. Weeks, *J. Res. Natl. Bur. Stand., Sect. A,* **66,** 13 (1962).
32. D. R. Beech and C. Booth, *J. Polymer. Sci. Polym. Lett. Ed.,* **8,** 731 (1970).
33. J. Brandrup and R. H. Immergut, *Polymer Handbook,* 3rd. Ed., Wiley Interscience, New York, 1989, Part V, p. 71.
34. S. Z. D. Cheng and B. Wunderlich, *J. Polym. Sci. Polym. Phys. Ed.,* **24,** 577 (1986).
35. D. R. Paul, J. W. Barlow, R. E. Bernstein, and D. C. Wahrmund, *Polym. Eng. Sci.,* **18,** 1255 (1978).
36. Y. Nishio, T. Haratani, and T. Takahashi, *J. Polym. Sci. Polym. Phys. Ed.* **28,** 355 (1990).
37. G. C. Alfonso and T. R. Russell, *Macromolecules,* **19,** 1143 (1986).